Worst-case Model for Calculation of Lightning Electromagnetic Field

Arlou Y.Y.*†, Tsyanenka D.A.*, Sinkevich E.V.* and Xie Ma‡
*EMC R&D Laboratory
Belarusian State University of Informatics and Radioelectronics
Minsk, Belarus
emc@bsuir.by
†Faculty of Radiophysics and Computer Technologies
Belarusian State University
Minsk, Belarus
orlovraf@gmail.com
‡China Electronics Technology Cyber Security Co., Ltd
18081045600@163.com

***Abstract*—A worst-case analytical model of electromagnetic field created by the lightning is developed. The model makes it possible to estimate magnitude, direction and spectra of electric and magnetic field intensity vectors in observation point. The model is intended for express analysis of EMC and immunity of radio and electronic equipment of complex systems. Lightnings with discharge channel between cloud and surface of Earth as well as cloud-to-cloud and intercloud lightnings are considered. The model is applicable for an arbitrary location of observation point. Validation of the developed model is carried out by comparison of results obtained in framework of the model with results of measurements and numerical simulations.**

***Index Terms*—lightning, electromagnetic interference, electromagnetic pulse propagation, electromagnetic fields, electromagnetic spectrum**

I. Introduction

Increase of number and complexity of equipment used in modern big systems (e.g., automobiles) leads to increased complexity of analysis and providing of electromagnetic compatibility and immunity of these systems to external electromagnetic disturbances. Models intended for express analysis of EMC (the main goal of express analysis is to exclude from analysis definitely not dangerous influence paths and spurious couplings) in big systems (e.g., aircraft, ship) [1], [2] and its immunity to electromagnetic disturbances [3] must have high computational efficiency and must guarantee a worst-case estimation in various conditions. Electromagnetic (EM) field of lightning is important to account for during EMC analysis because it could break down equipment without direct lightning strike [4].

Authors of the present paper do not know standards describing electromagnetic environment in order to measure immunity to electromagnetic pulse created by lightning. According to [4, p. 709], "Other than for aerospace systems, the level of lightning electromagnetic field is not usually standardized for testing equipment. The exception is the test defined in IEC 61000-4-9 which is intended mainly for equipment that might be near ground conductors on a building struck by lightning and equipment in exposed substations". In [5], disturbances in form of the specified current or voltage levels are used for testing. Exception is ordnance [6, p. 18], its normal function in exposed condition is required after near lightning strike, but only electric and magnetic field rate of change is specified for this strike [6, table 8].

There are big number of models of current distribution along the lightning channel [7]. Calculated current distribution can then be used to calculate electromagnetic field, e.g., numerically [8]. Models allowing computation of lightning electromagnetic field known to the authors have the following drawbacks: 1) Calculation of the lightning EM field by using computational electromagnetics methods are computationally expensive if compared to closed-form analytical expressions; 2) Model [9] does not allow computation by closed-form expressions at distances between near and far ranges and in cases when observation point is located at far range and height is comparable to distance between lightning and observation point; 3) In order to apply analytical solutions in frequency domain for calculation of electromagnetic field in time domain, it is required to use computationally-expensive (as compared to analytical solutions) inverse Fourier transform.

A model of lightning electromagnetic environment (EME) based on measurements exists [10]. In [10], measurement results of electric field peak amplitude E_{peak} and its peak rate of change $\frac{dE}{dt}_{peak}$ are given in table form. But, in order to analyze penetration of electromagnetic pulse in the system and change of its parameters (e.g., E_{peak} and $\frac{dE}{dt}_{peak}$) during penetration, it is necessary to consider and to analyze electromagnetic pulse waveform itself. Also, the model [10] is applicable for observation points placed near to Earth surface, and separate consideration is necessary for observation points placed at high altitudes. The model [10] was used to validate the developed model (see Section VI-A).

Similarly to [10], peak amplitude and rate of change are chosen as important parameters of electromagnetic pulse

DOI: 10.1109/EMCEurope.2018.8485075

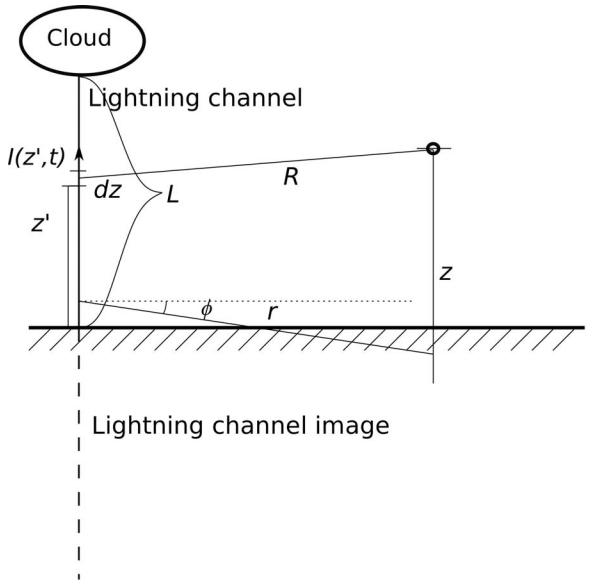

Figure 1. Geometrical configuration and coordinate system used during analysis of lightning between Earth surface and cloud. L is the length of the lightning channel; r, ϕ, z are coordinates of the observation point in cylindrical coordinate system; $I(z',t)$ is current in the lightning channel at height z' from Earth

waveform.

The objective of the paper is to develop a worst-case computationally-effective model of waveform and spectrum of lightning electromagnetic field. The model must be applicable for lightnings between a cloud and Earth surface and lightnings between clouds or parts of cloud, and for arbitrary observation points. Peak amplitude and rate of change for electric and magnetic fields computed by the model must not be underestimated.

II. Used Approximations and Simplifications

1) Calculation of the electromagnetic field is based of images method (see Fig. 1). Earth surface is approximated by a flat perfect electric conductor (the worst case). Exception is made for accounting of radial component existing due to finite conductivity of Earth [7].
2) Air is medium in which electromagnetic pulse of the lightning is propagated. It is supposed that the medium does not have dispersion and absorption.
3) Reflections from surrounding objects are not accounted (except for Earth surface; see i. 1).
4) Model of current distribution is transmission line (TL) model [9, eq.4]:

$$i(z',t) = u(t - z'/v) \cdot i(0, t - z'/v) \qquad (1)$$

where v is propagation speed of current pulse; $u(t - z'/v)$ is the Heaviside function.
5) Electrostatic field of charges in cloud is not accounted because it is not pulsed field.

III. Current in Lightning Channel

A. Lightning between Earth Surface and Cloud

Various shapes of lightning current pulse waveforms $I(t)$ are used in literature (see, e.g., [7]). In this paper, in the same way as in [6, p. 20], a model of double exponential pulse $I = I_0(e^{-\alpha t} - e^{-\beta t})$ is used, because precision of this expression is enough to solve problems of electromagnetic compatibility. Peak rate of change for double exponential pulse occurs when t=0 and is equal to $\frac{dI}{dt}_{peak} = I_0(\beta - \alpha) \approx I_0\beta$.

Accounting of electromagnetic fields created by the lightning is required for estimation of lightning indirect effects [6, p. 5]. A model [6, fig. 1, 2, table 7] defines current in lightning channel as sum of several components A, A_h, B, C, D, D/2, H. Each component is a double exponential pulse with specified parameters. In most cases, component A is the most dangerous. It has the following parameters $I_{A\,peak}$ ≈200 kA, α_A ≈11·10^3 s^{-1}, β_A ≈0.65·10^6 s^{-1}, $\frac{dI}{dt}_{A\,peak} \approx I_{A\,peak}\beta_A$=139 kA/us.

Peak current amplitude 200 kA given in [6] for severe stroke is worst-case, because lightnings with similar or higher amplitude are observed extremely rarely [10]. Probability distribution of peak current amplitude is given in [11, Table A.3], according to which probability of current exceeding 200 kA during lighting strike is only 1 %. Current in the lightning channel determines created EM field. In order to make cheaper protection from EM field of lightning, risk of underestimation can be increased and peak current amplitude used for computations can be decreased. For example, in [10], I_{peak} equal to 30 kA is given as typical and equal to 80 kA as extreme. [11, table A.3] can be used to choose peak current created by lightning, protection against electromagnetic field of which is developed.

Results of lightning current measurements are given in [10], according to which the worst case is I_{peak}=80 kA, $\frac{dI}{dt}_{peak}$=410 kA/us. 410 kA/us is large value; according to [11, p. 36], $\frac{dI}{dt}_{peak}$=200 kA/us, which is comparable to $\frac{dI}{dt}_{peak}$ for [6], therefore, $\frac{dI}{dt}_{peak}$ for [6] is used in the paper.

According to [10], $\frac{dI}{dt}_{peak}$ is equal to 110 kA/us for I_{peak}=30 kA. For MIL-STD 464C, $\frac{dI}{dt}_{peak}$=139 kA/us in case I_{peak}=200 kA. Weak dependency of $\frac{dI}{dt}_{peak}$ is confirmed by [12, table 1], according to which lightning pulses with greater peak amplitude has greater rise time. Therefore, we do not recommend to decrease peak rate of current rise while decreasing peak current during calculations. Parameter β can be estimated as $\frac{dI}{dt_{peak}}/I_0$. There is few data for I_{peak} and $\frac{dI}{dt}_{peak}$ in case of first return stroke, because rocket-triggered lightnings do not have first return stroke. According to [10], I_{peak} for first return stroke can be accepted as doubled I_{peak} for subsequent return stroke, and $\frac{dI}{dt}_{peak}$ can be accepted the same. $\frac{dI}{dt}_{peak}$ equal to 139 kA/us (from [6]) is used further.

Dependence of current pulse on time t can be written as follows:

$$I(t, I_0, \alpha, \frac{dI}{dt}_{peak}) = \begin{cases} 0 & if \ \ t < 0 \\ I_0(e^{-\alpha t} - e^{-t\frac{dI}{dt}_{peak}/I_0}) & else \end{cases} \quad (2)$$

Spectrum of pulse (2) is calculated at frequency f according to the following expression [13, eq. 10]:

$$\tilde{I}(f) = \frac{I_0(\frac{dI}{dt}_{peak}/I_0 - \alpha)}{(j2\pi f + \alpha)(j2\pi f + \frac{dI}{dt}_{peak}/I_0)} \quad (3)$$

where j is imaginary unit.

In case of low-Q systems, each lightning component can be considered independently. Component A has maximum spectrum up to 3 MHz, component H has maximum spectrum for higher frequencies (level of H component spectrum is about 50 % higher). So, in case of low-Q systems, it is necessary to use maximum among spectra of components A and H computed according to (3) using $\frac{dI}{dt}_{peak}/I_0 = \beta$ corresponding to the calculated component (parameters of pulses are given in [6, table 7]).

Necessity to estimate several lightning pulses as one waveform during spectrum calculation in case of high-Q systems can be estimated as follows. Time constant t_c of transient process damping for high-Q resonator with aperture and without absorber can be close to 1 us [14], and this is much less than minimal (worst-case) time interval between H-components equal to T_H =50 μs [6, fig. 2]. Input filter of subband 4 (500 kHz – 900 kHz) for AR 5000 receiver has pass bandwidth Δf_{3dB} equal to about 100 kHz in lower part of the subband [15, p. 74]. Estimation of transient process damping time for an ideal pass-band filter is $t_{0.05} \approx 6.4/\Delta f_{3dB}$=64 μs (under condition that EM field does not break down semiconductor elements used for electronic switching of the filter and the receiver subbands), and this is comparable with T_H. Therefore, it is necessary to consider several pulses of lightning H components as one waveform in come cases of high-Q systems. A worst-case model of the spectrum (amplitude envelope) for several H components is a sum of magnitudes of spectra of these components (3).

B. Lightning between Clouds or Parts of Cloud

Channel length of lightning between parts of cloud is about 5-10 km [8, p. 11]. In order to analyze EM pulse influence of lightning between clouds or parts of cloud, waveform of current corresponding to such lightnings is accepted to be equal to current waveform of lightning between cloud and Earth (2). This is a worst case, because [8, p. 11]: "The charge motion in cloud discharges produces electric fields whose frequency spectra have roughly the same amplitude distribution as those of ground discharges for frequencies below about 1 kHz and above about 100 kHz. Within the frequency band from 1 kHz and 100 kHz, the ground discharge is a more efficient radiator because of the very energetic return strokes". Similar data is given in [16, p. 254].

IV. EM Field of Lightning between Earth Surface and Cloud

A. Numerical Model

Waveform of electric and magnetic field in given observation point can be found for given time and spatial distribution of current in the lightning channel by the following expressions [9, eq. (2)], [8], [17]:

$$E_{z\,num} = \frac{1}{4\pi\varepsilon_0}\int_{-L}^{L}\left[\frac{2(z-z')^2 - r^2}{R^5}\int_0^t I(z', t' - \frac{R}{c})dt' + \right.$$
$$\left. + \frac{2(z-z')^2 - r^2}{cR^4} I(z', t - \frac{R}{c}) - \frac{r^2}{c^2R^3}\frac{\partial I(z', t - \frac{R}{c})}{\partial t}\right] dz' \quad (4)$$

$$E_{r\,num} = \frac{1}{4\pi\varepsilon_0}\int_{-L}^{L}\left[\frac{3r(z-z')}{R^5}\int_0^t I(z', t' - \frac{R}{c})dt' + \right.$$
$$\left. + \frac{3r(z-z')}{cR^4} I(z', t - \frac{R}{c}) + \frac{r(z-z')}{c^2R^3}\frac{\partial I(z', t - \frac{R}{c})}{\partial t}\right] dz' \quad (5)$$

$$H_{\phi\,num} = \frac{1}{4\pi}\int_{-L}^{L}\left[\frac{r}{R^3} i(z', t - \frac{R}{c}) + \frac{r}{cR^2}\frac{\partial i(z', t - \frac{R}{c})}{\partial t}\right] dz' \quad (6)$$

where $R = \sqrt{r^2 + (z-z')^2}$; ε_0 is electric constant; c is velocity of light in vacuum.

In general case, only numerical calculation according to (4)-(6) is possible using current distribution (2).

B. Near Region

At first, case $z, r \ll L$ is considered, current is directed from Earth to the cloud. 10 m is accepted as minimum distance from the lightning channel to the observation point (smaller distances must be interpreted as direct strike) [6, table 8, p. 87].

Linear charge density along the lightning channel:

$$\tau(z', t) = \int_0^t \frac{\partial}{\partial z'} i(z', t_a) dt_a = $$
$$= \int_0^t \frac{\partial}{\partial z'} i(0, t_a - z'/v) dt_a = $$
$$= \frac{1}{v}\int_0^t \frac{\partial}{\partial t_a} i(0, t_a - z'/v) dt_a = $$
$$= [\tau|_{t=0} = 0] = \frac{1}{v} i(L, t - z'/v) = \frac{1}{v} i(z', t) \quad (7)$$

Assumption that entire lightning channel has equal τ makes it possible to estimate upper bound of E_{peak} and $\frac{dE}{dt}_{peak}$. Problem geometry for the case of electric and magnetic fields

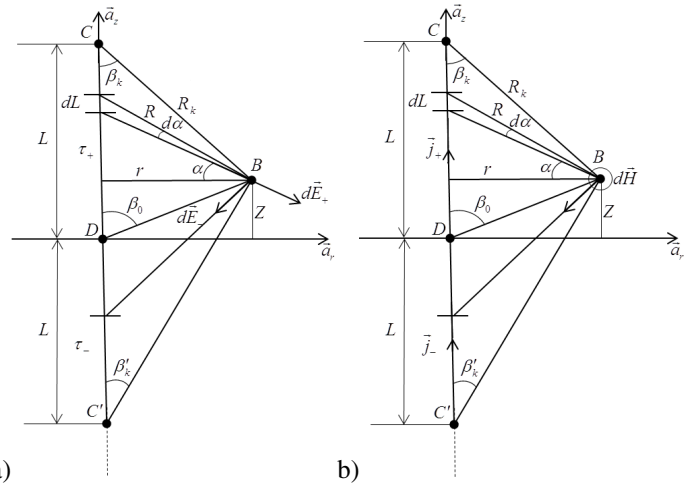

Figure 2. Illustration of quasistatic vectors of the electric and magnetic fields. Vector $\vec{a}_\varphi$ is directed inside the figure

computation is presented in Fig. 2. Resulting expressions for the electric field:

$$E_{qstat\ r} = \frac{I(t)\cdot(\cos\beta_k - \cos\beta'_k)}{4\pi\varepsilon_0 v\, r}; \quad \cos\beta_k, cos\beta'_k = \frac{L \mp Z}{\sqrt{(L\mp Z)^2 + r^2}}, \tag{8}$$

$$E_{qstat\ z} = -\frac{I(t)\cdot(\sin\beta_k + \sin\beta'_k - 2\sin\beta_0)}{4\pi\varepsilon_0 v\, r}; \quad \sin\beta_k, sin\beta'_k = \frac{r}{\sqrt{(L\mp Z)^2+r^2}}, \quad \sin\beta_0 = \frac{r}{\sqrt{Z^2+r^2}}; \tag{9}$$

Magnetic field in quasistatic approximation is calculated by the following expression:

$$H_{qstat\,\phi} \approx -\frac{1}{4\pi r} I(t)\,(\cos\beta_k + \cos\beta'_k) \tag{10}$$

The following simplified expressions are given in [9, eq. 19, 20] for the observation point placed at Earth surface in near region ($r \ll L$):

$$E_{near\ z} \approx -\frac{1}{2\pi\varepsilon_0 \nu r} I(t) \tag{11}$$

$$H_{near\ \phi} \approx -\frac{1}{2\pi r} I(t) \tag{12}$$

For observation points lying at Earth surface (z=0), equation (8) leads to zero result, and equations (9) and (10) in case $r \ll L$ are reduced to (11) and 12, respectively.

Values of the electric and magnetic fields calculated by (9)-(10) are increased with decrease of v. Value $v = c/2$ is accepted as the worst case.

In case when $Z \ll r$ is not satisfied, the field created directly by segments of the lightning channel with maximum linear charge density propagates to the observation point faster than the field created by images of these segments. Therefore, $E_{\ peak}|_{Z \gtrsim r}$ will be less than $E_{\ peak}|_{Z \ll r}$, and the worst-case assumption $z = 0$ can be used in case of absence of data about height of the observation point.

C. Far Region

According to [9, eq. (19), (20)], equations for far region ($R \approx r$, $r \gg L$) are as follows:

$$E_{far\ appr\ z} \approx -\frac{v}{2\pi\varepsilon_0 c^2 r} I(t) \tag{13}$$

$$H_{far\ appr\ \phi} \approx -\frac{v}{2\pi\, c\, r} I(t) \tag{14}$$

In case $z \gg r$, equations (13)-(14) are become too worst-case. In equation (4), component corresponding to $\frac{dI}{dt}$ creates the field in far-field region (without consideration of lightning channel image):

$$E_{far\ z\ CC}(z) = -\frac{1}{4\pi\varepsilon_0}\int_0^L \frac{r^2}{c^2 R^3}\frac{\partial I(z', t - R/c)}{\partial t} dz' \approx$$

$$\approx [I(z', t) = I(0, t - \frac{z'}{v}); R \approx R_k = \sqrt{r^2 + (L-z)^2}] \approx$$

$$\approx -\frac{r^2 v}{4\pi\varepsilon_0 c^2 R_k^3}\,[I(L, t - R_k/c) - I(0, t - R_k/c)] \tag{15}$$

The field of lightning with accounting of the channel image:

$$E_{far\ z\ GC}(z) = E_{far\ z\ CC}(z) + E_{far\ z\ CC}(-z) \tag{16}$$

Similarly for the other field components:

$$E_{far\ r\ CC}(z) = -\frac{1}{4\pi\varepsilon_0}\int_0^L \frac{r(z-z')}{c^2 R^3}\frac{\partial I(z', t - R/c)}{\partial t} dz' \approx$$

$$\approx -\frac{rzv}{4\pi\varepsilon_0 c^2 R_k^3}\,[I(L, t - R_k/c) - I(0, t - R_k/c)] \tag{17}$$

$$E_{far\ r\ GC}(z) = E_{far\ r\ CC}(z) + E_{far\ r\ CC}(-z) \tag{18}$$

$$H_{far\,\phi\,CC}(z) = \frac{1}{4\pi}\int_0^L \frac{r}{cR^2}\frac{\partial I(z', t - R/c)}{\partial t} dz' \approx$$

$$\approx -\frac{rv}{4\pi c R_k^2}\,[I(L, t - R_k/c) - I(0, t - R_k/c)] \tag{19}$$

$$H_{far\,\phi\,GC}(z) = H_{far\,\phi\,CC}(z) + H_{far\,\phi\,CC}(-z) \tag{20}$$

In case $r \gg z$, (16) is reduced to (13).

Comparison with results of numerical computations are showed that (16) are not always the worst-case. E.g., in case of L=7 km, z=20 km, r=100 m and any v, underestimation is about 10^4 and $\sim 1/r^2$. It is established that the component of (4) dominating in given region is component corresponding to $I(z', t - R/c)$ under spatial integral. According to calculations by (16), maximum rate of change of electrical field corresponds to $v = c$. Estimation of electrical field corresponding to $I(z', t - R/c)$ component in case of far region and $z \gg r$:

$$E_{far\,z\,CC\,axis}(z) = \\ = -\frac{1}{4\pi\varepsilon_0}\int_0^L \frac{2(z-z')^2 - r^2}{cR^4} I(z', t - R/c)dz' \approx \\ \approx [R \approx z - z'] \approx -\frac{1}{4\pi\varepsilon_0}\int_0^L \frac{2z^2}{cR^4} I(0, t - \frac{z-z'}{c} - \frac{z'}{v})dz' \approx \\ \approx [v = c] \approx -\frac{1}{4\pi\varepsilon_0}\int_0^L \frac{2z^2}{cR^4} I(0, t - \frac{z}{c})dz' \approx \\ \approx -\frac{1}{4\pi\varepsilon_0}\frac{2z^2 L}{cR_k^4} I(0, t - \frac{z}{c}) \quad (21)$$

$$E_{far\,r\,CC\,axis}(z) = \\ = \frac{1}{4\pi\varepsilon_0}\int_0^L \frac{3r(z-z')}{cR^4} I(z', t - R/c)dz' \approx \\ \approx [v = c] \approx \frac{1}{4\pi\varepsilon_0}\frac{3rzL}{cR_k^4} I(0, t - \frac{z}{c}) \quad (22)$$

$$H_{far\,\phi\,CC\,axis}(z) = \frac{1}{4\pi}\int_0^L \frac{r}{R^3} I(z', t - R/c)dz' = \quad (23)$$
$$\approx [v = c] \approx \frac{1}{4\pi}\int_0^L \frac{z}{R^3} I(0, t - \frac{z}{c})dz' \approx$$
$$\approx \frac{1}{4\pi}\frac{zL}{R_k^3} I(0, t - \frac{z}{c})$$

$$E_{far\,z\,GC\,axis}(z) = E_{far\,z\,CC\,axis}(z) + E_{far\,z\,CC\,axis}(-z) \\ E_{far\,r\,GC\,axis}(z) = E_{far\,r\,CC\,axis}(z) - E_{far\,r\,CC\,axis}(-z) \\ H_{far\,\phi\,GC\,axis}(z) = H_{far\,\phi\,CC\,axis}(z) + H_{far\,\phi\,CC\,axis}(z) \quad (24)$$

$v = c$ is used in the worst-case model in far region because, according to (13)-(14), this is the worst case.

D. Worst-Case Model

Due to the fact that Earth surface is not an ideal conductor, horizontal electric field is created for z=0 [7]. Expression $E_r = -I(t)/(2\pi r^2\sigma)$ [18, eq. 11.44], where σ is conductivity of the Earth, is used in the worst-case model with multiplier $(\cos\beta_k + \cos\beta_0)$ preventing huge overestimation in case of big z and small r.

Comparison with results of calculations according to (4)-(6) has shown that it is necessary to double expressions (15)-(20) in order to eliminate underestimation due to directed properties of lightning radiation. Minimum among doubled (15) and (13), and among doubled (20) and (14) is used in order to not overestimate field in case of $z \ll r$.

Final expressions for estimation of the lightning electric and magnetic field, applicable for an arbitrary observation point (including [7, eq. 11.48]):

$$E_{w\,z}(t) = \max(\left| E_{qstat\ z}|_{v=\frac{c}{2}} \right|, \left| E_{far\,z\,GC\,axis}(z)|_{v=c} \right| \\ + \min(2\left|E_{far\,z\,GC}(z)\right|, |E_{far\,appr\,z}|)) \quad (25)$$

$$E_{w\,r}(t) = \left|\frac{I(t)(\cos\beta_k + \cos\beta_0)}{2\pi r^2\sigma}\right| + \\ + E_{qstat\ z}|_{v=\frac{c}{2}} + 2E_{far\,r\,GC\,axis}(z) \quad (26)$$

$$H_{w\,\phi}(t) = \max(\left| H_{qstat\ \phi}|_{v=\frac{c}{2}} \right|, \\ \min(2\left| H_{far\,\phi\,GC}(z)|_{v=c} \right|, |H_{far\,appr\,\phi}|) \\ + |H_{far\,\phi\,GC\,axis}(z)|) \quad (27)$$

Eq. (2) with parameters I_A, α_A, $\frac{dI}{dt}_{peak} = I_A\beta_A$ from [6, table 7] must be used in (25), (26) and (27) as the worst case. Also, according to [7], the lowest σ=0.0001 S/m is used in (26).

According to (15)-(19), because always $I(z,t) \geq 0$, then $|I(L, t - R_k/c) - I(0, t - R_k/c)| \lessapprox |I(L, t - R_k/c)|$ and (15)-(19) will increase if one eliminate $I(0, t - R_k/c)$ in them. In this case, expressions (25)-(27) will be in direct proportion to the current, and spectrum of electromagnetic field can be estimated be replacing current in its equations by spectrum of the current calculated, e.g., by (3).

V. EM Field of Lightning between Clouds or Parts of Cloud

All expressions given above are applicable for this type of lightning if to eliminate part of electromagnetic field corresponding to image of the lightning channel (and to do transformation of coordinates, if it is necessary).

Expressions (8)-10 are changed as follows (electrostatic field of charged line):

$$E_{qstat\,z\,CC} = -\frac{I(t)}{4\pi\varepsilon_0 vr}(\sin\beta_k - \sin\beta_0); \quad (28)$$

$$E_{qstat\,r\,CC} = \frac{I(t)}{4\pi\varepsilon_0 vr}(\cos\beta_k + \cos\beta_0); \quad (29)$$

$$H_{qstat\,\phi\,CC} = H_{qstat\,\phi} \quad (30)$$

Summary expressions for the developed model:

$$E_{w\,z\,CC}(t) = \max(E_{qstat\ z\,CC}|_{v=\frac{c}{2}}, |E_{far\,z\,CC\,axis}(z)| \\ + 2\,E_{far\,z\,CC}(z)|_{v=c}) \quad (31)$$

$$E_{w\,r\,CC}(t) = E_{qstat\ r\,CC}|_{v=\frac{c}{2}} + \\ + 2E_{far\,r\,CC}(z) + E_{far\,r\,CC\,axis}(z) \quad (32)$$

$$H_{w\,\phi\,CC}(t) = \max(H_{qstat\ \phi\,CC}|_{v=\frac{c}{2}}, H_{far\,\phi\,CC\,axis}(z) \\ + 2\,H_{far\,\phi\,CC}(z)|_{v=c}) \quad (33)$$

Table I
MEASURED AND COMPUTED CHARACTERISTICS FOR ELECTRIC FIELD INTENSITY: [1] [10], TYPICAL; [2] [10], EXTREME; [3] EXPRESSION (25); [4] [6, TABLE 8].

	r, m	10	30	50	110	500	$100{\cdot}10^3$
1	$E_{peak\,typ}$ [1], kV/m	97	35	28	13	2.0	0.0086
2	$E_{peak\,ext}$ [2], kV/m	174	62	36	16	2.6	0.020
3	$E_{peak}\vert_{I_0=30kA}$ [3], kV/m	360	120	71	32	6.7	0.020
4	$\frac{dE}{dt}_{peak\,ext}$ [2], kV/m/us	680[4]	226	292	-	-	0.1
5	$\frac{dE}{dt}_{peak}\vert_{I_0=30kA}$ [3], kV/m/us	1664	553	331	149	31	0.923

VI. VALIDATION OF WORST-CASE MODEL

A. Comparison with Measurement Results

The model [10] was used as a source of measurement results. Rate of change for electric field is approximately equal for the first and subsequent return stroke [10]. Therefore, it is possible to consider only waveform of first return stroke.

Results of comparison of the model [10] and the developed model are presented in table I. It can be seen that values in rows 3 and 5 computed by the model (25) are more or slightly less than values given in rows 1-2 and 4, respectively. Value of 30 kA instead of 80 kA (80 kA corresponds to the extreme case according to [10]) is used as peak current amplitude for (25), therefore, table I demonstrates the worst-case behavior of the developed model. Notes: Values of table II from [10] corresponding to row "E-field peak (V/m)" are interpreted as kV/m.

B. Validation by Numerical Calculation

Expressions (4) and (6) were programmed in jupyter notebook (python), and waveforms of electric and magnetic fields, E_{peak}, $\frac{dE}{dt}_{peak}$, H_{peak} and $\frac{dH}{dt}_{peak}$ were calculated for the following values of parameters: v=[0.5c; 0.7c; 0.9c; c], r=[10 m; 50 m; 100 m; 500 m; 1 km; 10 km; 100 km], L=[2, 7.5 km], z=[0; 10 m; 50 m; 100 m; 500 m; 1 km; 10 km; 100 km] (the program in jupyter and calculation results are available at https://drive.google.com/drive/folders/1L6fT79e6UI4KE6QNylaFclpahXm4wZeb?usp=sharing).
The fields that are changed slowly comparatively to current did not accounted. Almost all E_{peak}, H_{peak}, $\frac{dE}{dt}_{peak}$ and $\frac{dH}{dt}_{peak}$ derived numerically are lower or insignificantly higher than corresponding values computed by (25)-(27). Exceptions: high spikes of electromagnetic field with big amplitude of the derivative are found in case of $Z \gg L$, $v \geq 0.9c$, $Z \gg r$ (this effect is noted in [7]), and the developed model don't account for these spikes. Also, in some cases, underestimation of one of field components is noted (absolute value of the electric field vector is estimated correctly).

VII. CONCLUSION

The worst-case model of electromagnetic field created by the lightning is developed. The model is applicable for all heights of observation points and distances to lightning. Electric field calculated by the model can be used for modeling of lightning electromagnetic pulse impact on equipment of complex systems. Spectrum of electric and magnetic field can be estimated by substitution of lightning channel current spectrum into the developed model (eqs. (25), (26) and (27)).

Developed worst-case model can be applied for diagnostics (express analysis) of EMC and immunity of radio and electronic equipment of complex systems.

The model does not account for processes occurring during lightning near to clouds. Directions of further development of the model: to account for spikes in case of $Z \gg L$, $v \geq 0.9c$, $Z \gg r$.

REFERENCES

[1] J. L. Bogdanor, R. A. Pearlman, and M. D. Siegel, Intrasystem Electromagnetic Compatibility Analysis Program: Volume I – User's Manual Engineering Section. Mc.Donnel Douglas Aircraft Corp., Rome Air Development Center, Griffiss AFB NY, Dec. 1974.

[2] E. V. Sinkevich, V. I. Mordachev, and et al., "Emc-analyzer. mathematical models and algorithms of electromagnetic compatibility analysis and prediction software complex," Tech. Rep., 2018.

[3] F. Eriksen, T. Rudolph, and R. Perala, "Atmospheric electricity hazards analytical model development and application. volume 3: Electromagnetic coumpling modeling of the lightning/aircraft interaction event," Final Report, Aug. 1979-Jun. 1981 Electro Magnetic Applications, Inc., Denver, CO., 1981.

[4] Y. Chen, H. Wan, and X. Zhou, "Simulation of lightning electromagnetic fields and application to immunity testing," IEEE Transactions on Electromagnetic Compatibility, vol. 57, no. 4, pp. 709–718, 2015.

[5] RTCA/DO-160G. Environmental Conditions and Test Procedures for Airborne Equipment, RTCA, Inc. Std., December 2010.

[6] MIL-STD-464C. Electromagnetic environmental effects. Requirements for systems, Department of Defense Std., October 2010.

[7] V. Cooray, The lightning flash. The Institution of Engineering and Technology, 2014.

[8] M. A. Uman and E. P. Krider, "Atmospheric electricity hazards analytical model development and application. volume i. lightning environment modeling." ELECTRO MAGNETIC APPLICATIONS INC DENVER CO, Tech. Rep., 1981.

[9] Y. Chen, H. Wango, and V. A. Rakov, "Analysis of lightning electromagnetic fields at near and far ranges," in XV International Conference on Atmospheric Electricity, Norman, USA, 2014.

[10] R. Thottappillil, "Electromagnetic pulse environment of cloud-to-ground lightning for emc studies," IEEE Transactions on Electromagnetic Compatibility, vol. 44, no. 1, pp. 203–213, 2002.

[11] IEC 62305-1. Protection against lightning. Part 1: General principles, IEC Std., 2010.

[12] N. A. Ahmad, M. Fernando, Z. Baharudin, M. Rahman, V. Cooray, Z. Saleh, J. R. Dwyer, and H. K. Rassoul, "The first electric field pulse of cloud and cloud-to-ground lightning discharges," Journal of Atmospheric and Solar-Terrestrial Physics, vol. 72, no. 2, pp. 143 – 150, 2010.

[13] IEC 61000-2-9. Part 2: Environment - Section 9: Description of HEMP environment - Radiated disturbance. Basic EMC publication, IEC Std., 1996.

[14] D. A. Hill, M. T. Ma, A. R. Ondrejka, B. F. Riddle, M. L. Crawford, and R. T. Johnk, "Aperture excitation of electrically large, lossy cavities," IEEE transactions on Electromagnetic Compatibility, vol. 36, no. 3, pp. 169–178, 1994.

[15] AR5000. Service Manual, AOR Ltd., Tokyo, 1997.

[16] MIL-HDBK-274. Electrical grounding for aircraft safety, Naval air systems command Std., December 1983.

[17] D. W. P. Thomas, C. Christopoulos, and E. T. Pereira, "Calculation of radiated electromagnetic fields from cables using time-domain simulation," IEEE Transactions on Electromagnetic Compatibility, vol. 36, no. 3, pp. 201–205, Aug 1994.

[18] V. Cooray, Lightning electromagnetics. The Institution of Engineering and Technology, 2012.